

6.1

A Discretely Propagating Nocturnal Oklahoma Squall Line: Observations and Numerical Simulations

Robert G. Fovell*, Brendon Rubin-Oster and Seung-hee Kim
University of California, Los Angeles

1. Introduction

Many common storms, such as squall lines, propagate because they precipitate. More precisely, some of the precipitation evaporates before reaching the surface, establishing a subcloud cold pool that spreads along the ground. This pool helps lift moist, low-level air into the storm at its leading edge or gust front. Even though the ascent tends to get temporally punctuated into individual convective cells, this mechanism has become known as continuous propagation. The continuity is provided by the spreading cold pool's persistence.

Yet, radar imagery often reveals new storms firing up in advance of established convection, particularly near nocturnal squall lines. If the new cells appear out ahead of the gust front, a mechanism other than cold pool lifting is operating. Many of these new cells appear to subsequently merge with the main convective line, frequently resulting in a temporary strengthening of the established storm. However, more rapid development acts to weaken the original convection by blocking its inflow. In the latter case, a fundamentally discrete mode of propagation is accomplished. In general, we will refer to the establishment of new cells out ahead of the line as discrete initiation.

A particularly good example of discrete initiation was afforded by the roughly north-south oriented squall line that entered Oklahoma from the west in the early morning hours of 21 June 2003. Figure 1 shows base reflectivity recorded by the Vance Air Force Base (VNX) radar at about 0615 and 0637Z. The latter time reveals that a discrete line of new cells, residing roughly 40 km ahead of the storm's main echo mass, had appeared during the preceding twenty minutes. This separation distance, though large, does not by itself preclude the gust front mechanism. However, the surface temperature analyses from the Oklahoma Mesonet (superposed) and the appearance of a radar fine line (see arrow at right) place the gust front well to the west of the new convection.

Indeed, Fig. 2, showing reflectivities for 0700Z and 0724Z, the gust front can be seen first approaching and then un-

derunning the new line. The circle at right marks a cell that evinced a marked increase in reflectivity as the gust front passed beneath it. New, discretely initiated lines of cells continue to appear ahead of the squall line as it propagates eastward (Fig. 3). Note the new lines share a common northwest-to-southeast (NW-SE) alignment, making an acute angle to the rather more north-south oriented main storm.

Below, we offer speculation regarding initiation mechanisms for the systematic development of discrete new cell lines and the factors influencing their characteristic NW-SE alignment.

2. An MM5 simulation

Figure 4 presents results from an MM5 simulation employing a single 1320x1000 km domain at 4 km resolution. Runs using telescoping meshes with convective parameterizations active in the coarser grids were less successful in simulating this case. The simulation was initialized from Eta model reanalyses and utilized Reisner 2 microphysics and the MRF boundary layer parameterization. This MM5 run saw the establishment of an organized line that propagated into Oklahoma during the early morning hours. The cloud water (isosurface), water vapor field at 2 m (colored) and 10 m wind (vector) fields are shown at around 0300Z (2200 local time), when the squall line was still in the Texas Panhandle.

In contrast with the real case, the simulated squall line weakened after local midnight and was oriented northeast-southwest. This was perpendicular to the horizontal winds and the vertical wind shear in the lowest ≈ 400 m, according to the hodograph from Atmospheric Radiation Measurement (ARM) Southern Great Plains (SGP) site in north-central Oklahoma (Fig. 5). The actual squall line was perpendicular to the vertical shear between roughly 0.5-1.5 km, which was directed eastward.

Note in Fig. 4 the presence of NW-SE oriented bands in the model's surface moisture field. These bands appeared earlier in the simulation, the result of horizontal convective roll (HCR) activity in the model boundary layer. The NW-SE alignment of the HCRs corresponded to the direction of the shear (and winds) within the very lowest (≈ 400 m) layer. Figure 6 shows a vertical cross-

*Corresponding author address: Robert Fovell, UCLA Atmospheric and Oceanic Sciences, Los Angeles, CA 90095-1565. E-mail: rfovell@ucla.edu.

section taken perpendicular to the roll axes at 0015Z or 1915 local time. The rolls were undoubtedly excited by the development of a shallow superadiabatic layer immediately above the ground surface (visible in the figure) during the afternoon hours. The rolls dissipated as the surface cooled during the evening but, as revealed by Fig. 4, the spatial pattern of moistening and drying by their updrafts and downdrafts persisted for several hours longer.

Visible satellite imagery (Fig. 7) reveals there *were* HCRs, manifested by low-level roll clouds, over the area of interest during the previous afternoon. The model's HCRs, however, are undoubtedly spurious. Kuettner (1971) determined that thermally forced HCRs should have wavelengths of roughly three times the boundary layer depth, a length scale that would be unresolvable at the model resolution employed herein. The actual roll clouds had a roughly 8 km spacing; the MM5 model's rolls had far larger separations. Further, the model's boundary layer scheme should be generating the vertical mixing the rolls were created to accomplish. The rolls appeared, however, because the MRF parameterization was unable to prevent the development of the shallow superadiabatic layer.

Compared to the SGP hodograph (Fig. 5), model simulations indicate this southeasterly shear was present over a rather deeper layer earlier in the day and farther to the west, when and where the roll clouds actually formed. Still, we wondered if rolls could organize in an environment with the substantial directional shear exhibited in the SGP winds. We made an idealized simulation using ARPS initialized with this wind profile and the afternoon sounding from the same location. Horizontal homogeneity was broken through the inclusion of random perturbations to the surface fluxes. The model developed deep HCRs oriented NW-SE along the very low-level shear vector (not shown), despite the thin depth of that layer.

3. Discussion

The systematic development of lines of new cells in advance of the squall line is strong circumstantial evidence that the organized storm itself plays a major role in these new discrete developments. Of particular interest is the pronounced tendency for the new cell lines to adopt an orientation that is not directly parallel to the oncoming squall line. The spurious roll development in the MM5 is actually a fortuitous result as it suggested a mechanism for this orientation. It is hypothesized that roll activity in SW Oklahoma the previous afternoon worked to establish quasi-stationary bands in the moisture field that was able to persist into the morning hours. Naturally, the moistened zones residing in and above the roll updrafts would represent the more favorable locations for subsequent convection. Though lines of new cells comparable to the observations failed to appear in the simulation (see below), Fig. 5 shows that isolated new cells

occasionally appeared ahead of the gust front, initially collocated with the preexisting moisture bands.

It remains to identify a triggering mechanism that can act at a distance from the squall line. One possibility is that squall line's cold pool generated an undular bore in the act of propagating into a stable nocturnal boundary layer (e.g., Crook 1988). This bore would have progressed ahead of the main line, possibly providing crucial lifting to the moisture bands from below. We have thus far been unable to detect a bore signature in the available radar or mesonet data. Figure 8 shows a time series of surface air temperature and pressure from the Watonga station, located between the squall and new cell lines (see red dot in Fig. 1). A bore emanating from the oncoming storm would likely have crossed this station if it were responsible for instigating the new line that appeared to the east. Pressure generally decreased up until the gust front passed. There were undulations superposed on this decline, but they were very small amplitude, and not immediately suggestive of bore activity.

Another potential source of lifting could come from internal gravity waves (IGWs), trapped beneath the forward anvil. IGWs can be excited by temporal variations of convective heating in the squall line. Fovell and Kim (2003) showed that those waves can be ducted beneath the anvil owing to its characteristic decrease in stability and jet-like wind profile. In their simulation, the IGW amplitude was largest in the midtroposphere, with but a very slight surface signature. Thus, the presence of such waves probably cannot be confirmed from the mesonet surface data, though it is possible IGWs were responsible for Fig. 8's aforementioned minor pressure undulations.

Either of the above triggers could have been assisted, or even obviated, by the presence of a "moist tongue" of the type described by Fovell (2002). The moist tongue is a layer of increased humidity residing in the lower troposphere and extending out ahead of the squall line. It represents a very long period gravity wave response to the vertical distribution of heating in the storm's convective region. It is not known if this feature was present in the observations, but a well-developed moist tongue did appear in the MM5 simulation.

Figure 9 shows a vertical cross-section from this simulation (Fig. 4) roughly oriented along a moisture band and perpendicular to the squall line itself. The colored area shows local change of vapor mixing ratio over the past hour, with warm colors indicating moistening. A pronounced tendency for vapor mixing ratios to rise well in advance of the squall line is apparent in panel (a), with the largest moistening roughly 2.5 km above ground level. The tongue propagates with the squall line, so it isn't merely a result of the sloping terrain. Instead, it indicates the presence of persistent if gentle ascent in the storm's immediate inflow environment.

The superposed blue contours show condensate mixing ratios. A new cloud has just appeared in the tongue, about 70 km ahead of the gust front, at this time. This cloud develops into deep convection over the next 1.25 hours (Fig. 9b), prior to the gust front reaching this location. The new storm temporarily interrupts the moist tongue, in a similar manner as found by Fovell and Kim (2003).

Ducted IGWs do not appear in the MM5 simulation, probably owing to the absence of a well-developed forward anvil in the model storm (see condensate contours in Fig. 9). In contrast, the observed storm had a substantial leading anvil, and the new cell lines invariably appeared beneath the upper level cloud shield. This is shown by Fig. 10, which superposes radar and enhanced infrared satellite imagery at a time in which two parallel lines existed ahead of the squall line (see heavy black lines). The two lines reside beneath the forward anvil, and thus conditions favorable for IGW ducting could have been present in this case. It is believed that had the model storm developed a more realistic leading anvil, it would have been more successful in generating new clouds along the moisture bands.

Figure 11 utilizes an idealized, dry model to illustrate how IGWs and the moist tongue could have synergistically combined to establish new convection on the storm's forward side. The colored field is perturbation potential temperature (red indicating warming); vertical velocity is contoured. Panel (a) shows the response to maintained heating confined to a finite area. An essentially steady updraft is produced along with upper tropospheric warming stretching on either side of the heat source. Much of the latter was established by deep, compensating subsidence that had already passed out of the subdomain depicted by the time shown. Lower tropospheric cooling is seen stretching some 30 km ahead on the right, representing the storm's forward side, established by gentle lifting propagating in the wake of the deep subsidence. That same gentle lifting transports vapor up from the boundary layer, forming the moist tongue.

The effect of temporally varying heating associated with unsteady convection was investigated by forcing the maintained heat source to oscillate at a reasonable period (20 min) and amplitude ($\pm 25\%$). Short period IGWs which propagated within an environment modified by the time-mean heating were excited (Fig. 11b). Superposition of IGW-associated lifting in the moist tongue can bring about local areas especially favorable for convection (marked "X" on figure). As described in Fovell and Kim (2003), if clouds established in this fashion can become positively buoyant, they will be carried towards the storm by the lower tropospheric winds, possibly developing into deep convection prior to merging with the established storm.

4. Summary cartoon

We summarize with the help of Fig. 12, which illustrates a viable hypothesis for the generation and orientation of discretely generated bands of new cells aligned at an acute angle to the advancing squall line. It is acknowledged that the hypothesis is very speculative.

Figure 12a depicts moisture bands (red = more moist) oriented along the low-level shear vector. These lower tropospheric bands were the residual signature of HCR activity on the previous afternoon. It is not known how long such bands would persist following the disappearance of the roll circulations. However, it is reasonable to presume they would outlast the bands (spuriously generated) in the MM5 simulation, as the model is known to be somewhat overly diffusive. Thus, the bands could have been present in the early morning hours, when the new cell lines were observed to form ahead of the squall line in western Oklahoma.

That squall line is seen as causing two alterations in the environment into which it is propagating. Long-period gravity waves responding to persistent heating and cooling in the convective region help establish the lower-tropospheric moist tongue depicted in Fig. 12b. Temporal variations in this heating due to cellular activity excite short-period IGWs which, if trapped beneath the forward anvil, can travel well ahead of the squall line (Fig. 12c). These mechanisms, acting singly or in concert, can provide the "action at a distance" mechanism required to establish lines of new convective activity on the squall line's forward side. As illustrated in Fig. 12d, either trigger should result in new cells forming first along the nearer section of the moisture band, which would then develop outward along the band as the storm neared and/or the IGWs traveled farther.

Further research will explore this hypothesis with both idealized models and still more sophisticated real-data simulations. Hopefully, further supporting observational evidence will be forthcoming.

Acknowledgments. This work was supported by NSF grant ATM-0139284.

References

- Crook, N. A., 1988: Trapping of low-level internal gravity waves. *J. Atmos. Sci.*, **45**, 1533-1541.
- Fovell, R. G., 2002: Upstream influence of numerically simulated squall-line storms. *Quart. J. Roy. Meteor. Soc.*, **128**, 893-912.
- Fovell, R. G., and S.-H. Kim, 2003: Discrete Propagation in Numerically Simulated Nocturnal Squall Lines. Preprints, 10th Conf. on Mesoscale Processes, American Meteorological Society, unnumbered.
- Kuettner, J. P., 1971: Cloud bands in the earth's atmosphere: Observations and theory. *Tellus*, **23**, 404-426.

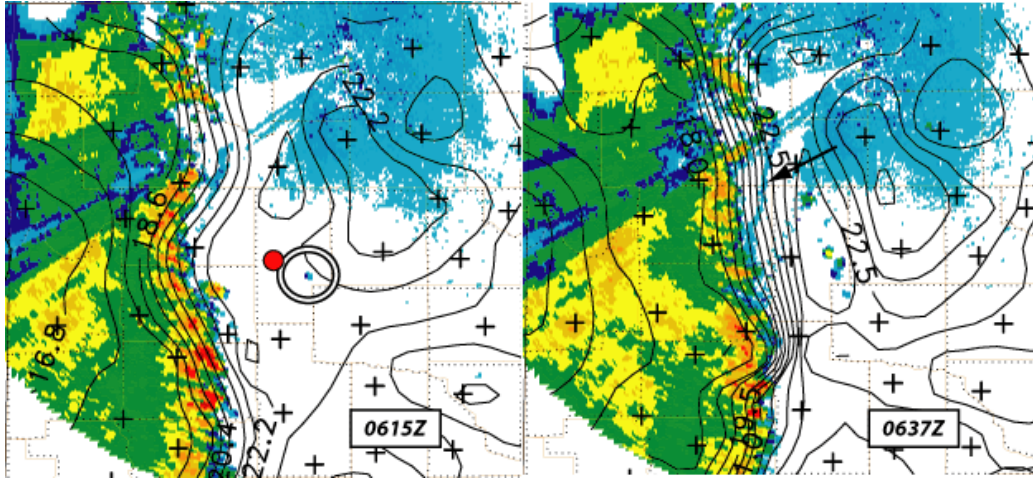


Fig. 1: Base reflectivity recorded by the Vance Air Force Base (VNX) radar around 0615Z and 0637Z on 21 June 2003, with surface temperature analyses (0.6°C contours) from the Oklahoma Mesonet data. Circle at left marks first echo to appear along new discrete line present in right-hand panel; arrow at right points out gust front. Plus signs mark mesonet station locations; red dot represents Watonga.

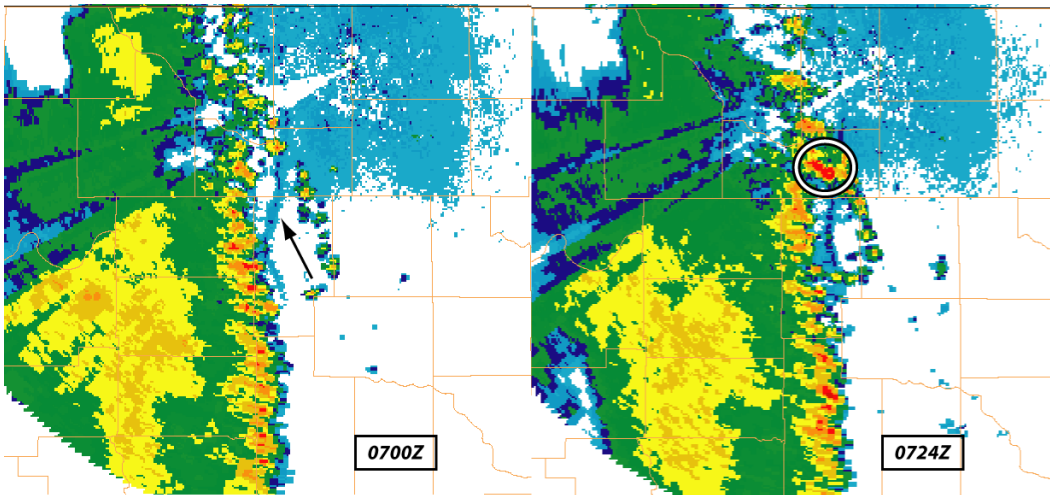


Fig. 2: VNX radar base reflectivity scans for two subsequent times, 0700Z and 0724Z. Arrow marks surface gust front position at 0700Z. Note intensification that occurs as gust front underruns one of the discretely-established new cells (circle, at right).

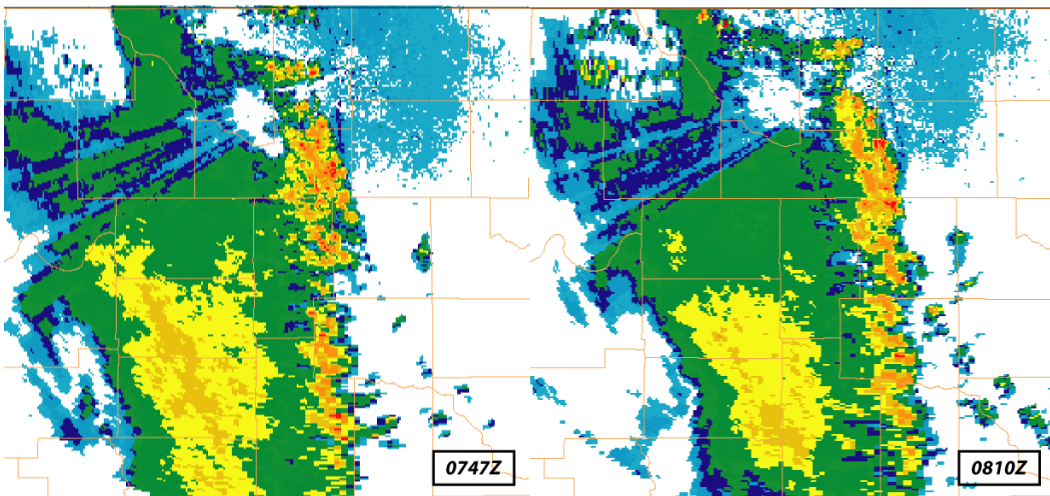


Fig. 3: As in Fig. 2, but for 0747Z and 0810Z. Note northwest-to-southeast orientation of successive discretely initiated lines.

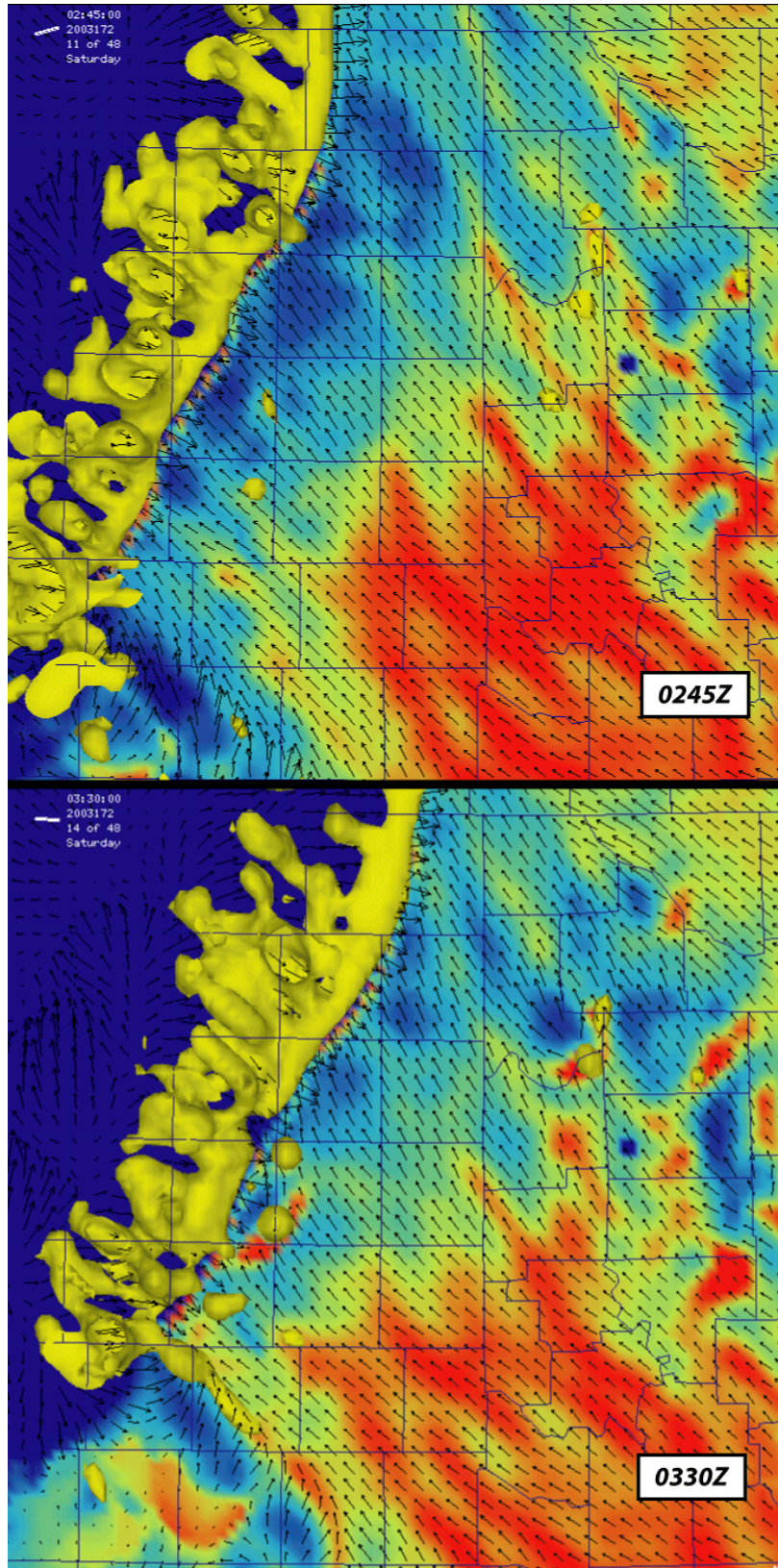


Fig. 4: Cloud water (0.5 g kg^{-1} isosurfaces), 2 m water vapor field (colored) and 10 m wind vectors for two times during an MM5 simulation. Fields are for the late evening hours of 20 June, when the squall line was still in the Texas Panhandle.

ARM/SGP radiosonde hodograph, 0531Z

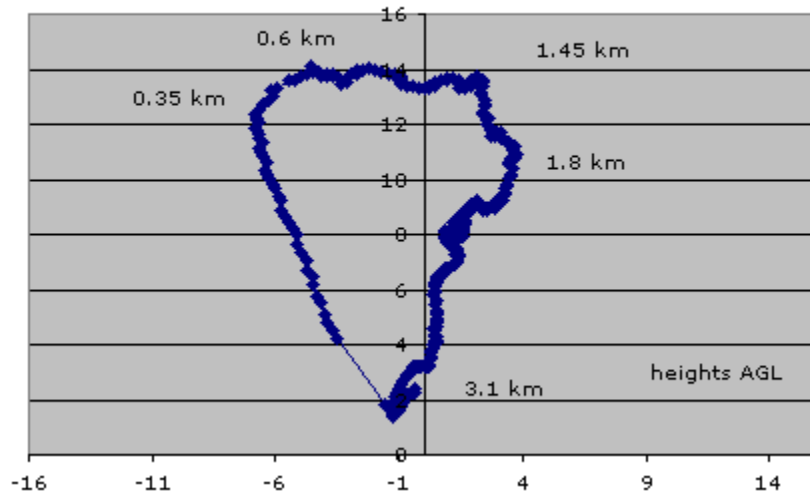


Fig. 5: Hodograph from ARM Southern Great Plains site C1, launched at 0531Z. Height labels are above ground level.

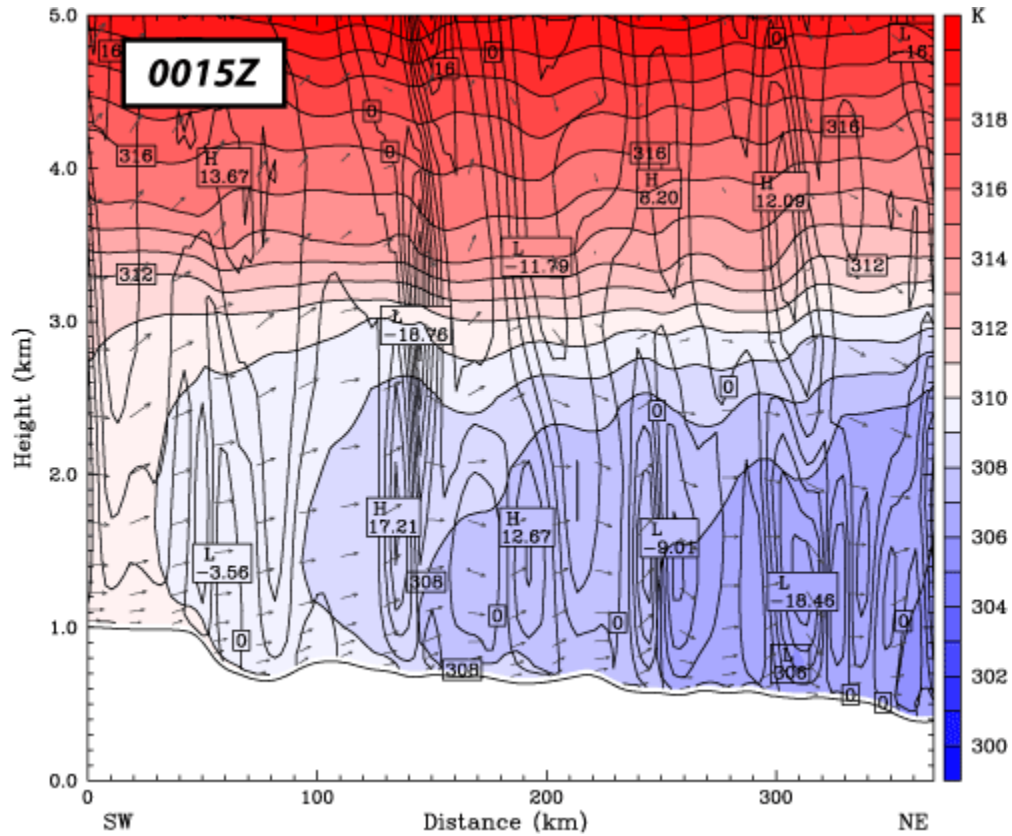


Fig. 6: Vertical cross-section, oriented SW-NE perpendicular to the near-surface vertical shear vector, showing potential temperature (colored) and vertical velocity (0.04 m s^{-1} contours) along with vector winds.

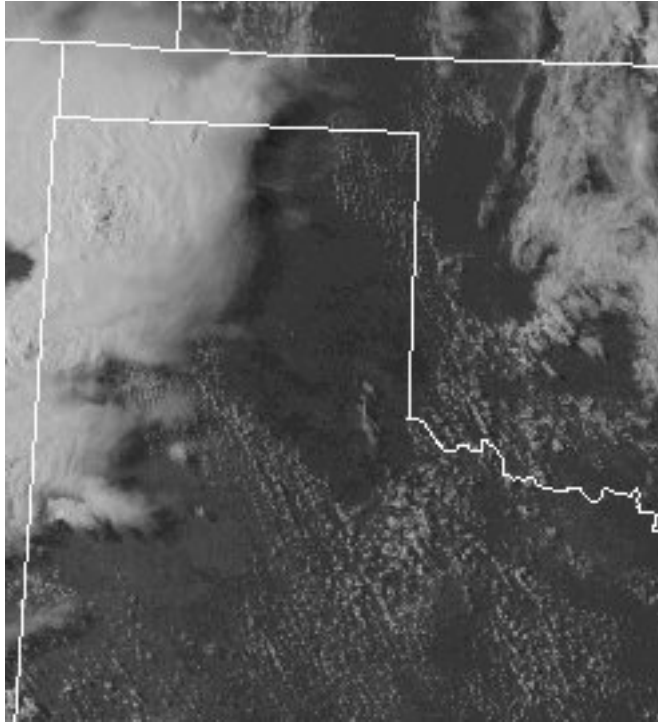


Fig. 7: Visible image from 2245Z (1745 local) on 20 June 2003, revealing NW-SE oriented cloud bands present over the Texas Panhandle and SW Oklahoma on the afternoon prior to the squall line passage. The developing line can be seen to the west.

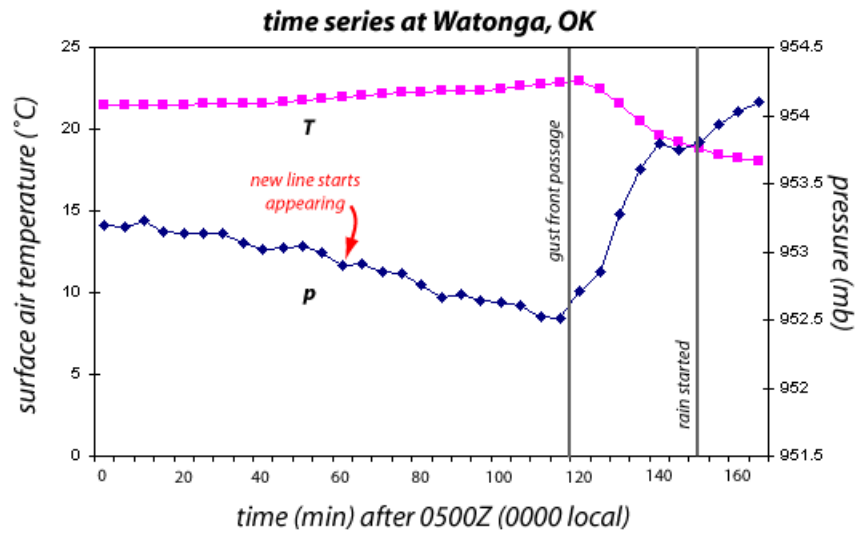


Fig. 8: Time series of surface air temperature (°C) and pressure (mb) from the Watonga mesonet station. See red dot on Fig. 1 left panel for location.

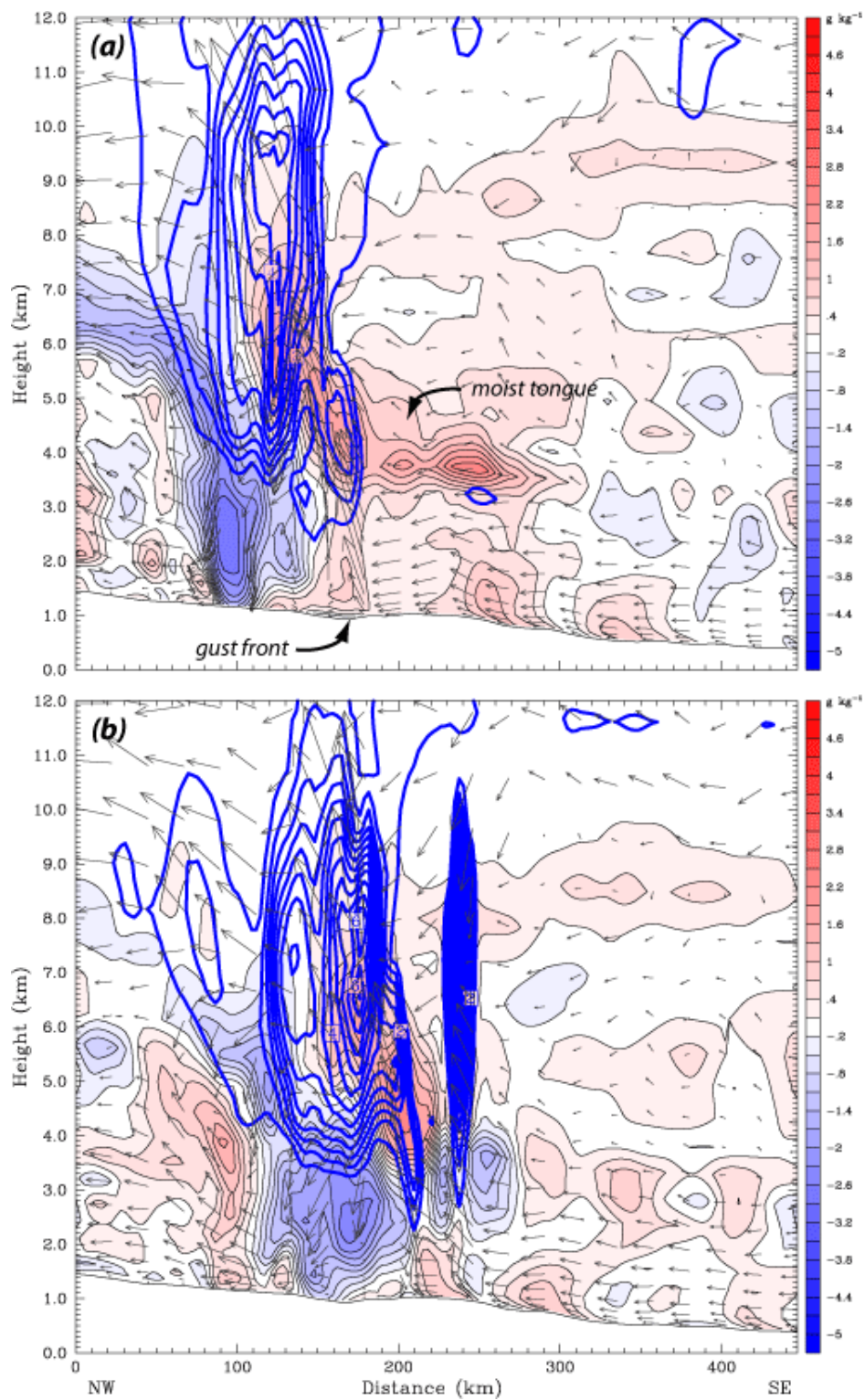


Fig. 9: A vertical cross-section from the MM5 simulation shown in Fig. 4, taken roughly along a roll axis, showing local change in the water vapor field over the previous hour (colored), superposed with 0.5 g kg^{-1} condensate contours and ground-relative winds, at 0215 and 0330Z.

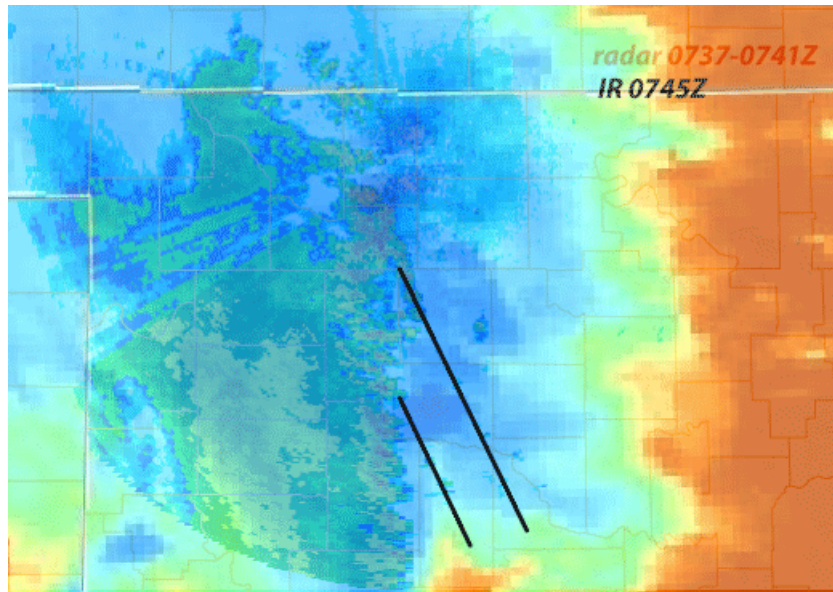


Fig. 10: VNX radar reflectivity superposed with enhanced infrared satellite imagery for approximately 0740Z. Parallel black lines denote locations of new cell lines present ahead of the main squall line at this time.

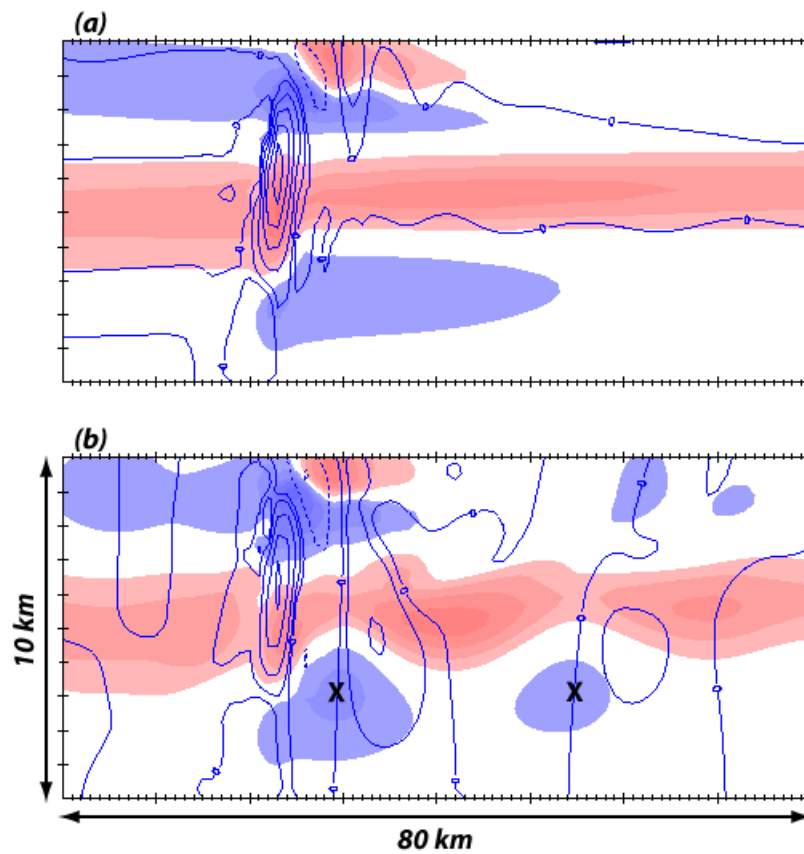


Fig. 11: Response to (a) maintained and (b) oscillating heat sources in an idealized model. Potential temperature perturbation relative to initial state (colored, red = warming) superposed with vertical velocity contours. "X" marks prime convective initiation locations.

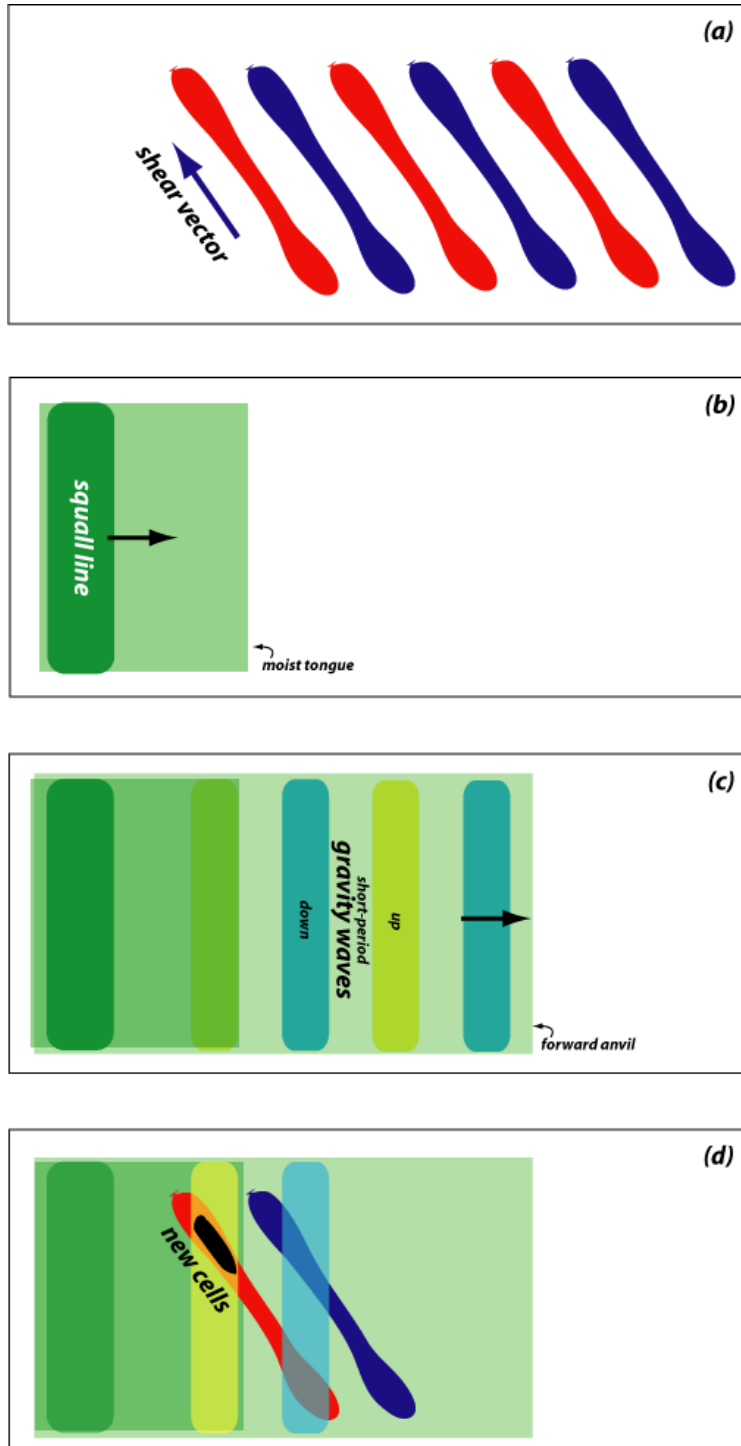


Fig. 12: Hypothesis for the development and orientation of new, discrete lines of convection ahead of an advancing squall line. In (a), afternoon convective rolls oriented parallel to the low-level shear vector leave behind bands of higher (red) and lower (blue) humidity that persist for hours after roll decay. The squall line depicted in (b) is propagating eastward, establishing a lower-tropospheric moist tongue in its inflow environment. Also excited are vertically trapped internal gravity waves that propagate ahead of the system beneath the forward anvil, depicted in (c). These waves are parallel to the squall line. As shown in (d), the extra lifting provided by the waves as they pass over the moisture bands could be responsible for generating new convection. When the waves and bands are not parallel, as is the present case, convection should form first on the band closer to the squall line and develop outward along the band with time, particularly as the moist tongue passes overhead. Dissipation of the gravity wave along with the finite extent of the moist tongue combine to favor convective initiation closer to the line rather than farther from it.